ACS APPLIED MATERIALS & INTERFACES

www.acsami.org

Research Article

DNA Hydrogels with Programmable Condensation, Expansion, and Degradation for Molecular Carriers

Kyounghwa Jeon, Chanseok Lee, Jae Young Lee, and Do-Nyun Kim*

Cite This: *ACS Appl. Mater. Interfaces* 2024, 16, 24162−24171

Read Online

ACCESS | Metrics & More | Article Recommendations | Supporting Information

ABSTRACT: Molecular carriers are necessary for the controlled release of drugs and genes to achieve the desired therapeutic outcomes. DNA hydrogels can be a promising candidate in this application with their distinctive sequence-dependent programmability, which allows precise encapsulation of specific cargo molecules and stimuli-responsive release of them at the target. However, DNA hydrogels are inherently susceptible to the degradation of nucleases, making them vulnerable in a physiological environment. To be an effective molecular carrier, DNA hydrogels should be able to protect encapsulated cargo molecules until they reach the target and release them once they are reached. Here, we develop a simple way of controlling the enzyme resistance of DNA hydrogels for cargo protection and release by using cation-mediated condensation and expansion. We found that DNA hydrogels condensed by spermine are highly resistant to enzymatic degradation. They become degradable again if expanded back to their original, uncondensed state by sodium ions interfering with the interaction between spermine and DNA. These controllable condensation, expansion, and degradation of DNA hydrogels pave the way for the development of DNA hydrogels as an effective molecular carrier.

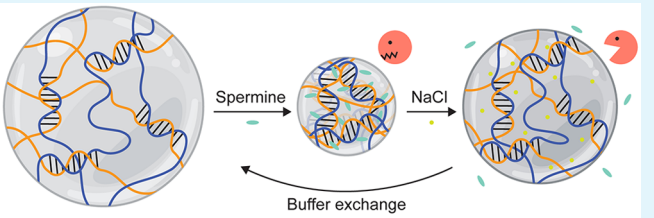

KEYWORDS: *DNA hydrogel, molecular carrier, stimuli responsiveness, volume change, enzyme resistance*

INTRODUCTION

Targeted molecular carriers have attracted attention to drug and gene delivery systems to avoid conventional drug administration requiring frequent and high dosages for therapeutic efficacy.[1,2] For the successful delivery of biological molecules, these carriers must robustly protect the cargo from biodegradation and other potential adversities[3] while responsive to environmental stimuli, for the targeted release of it. Hydrogels have gained increasingly more interest in this purpose due to their unique biocompatibility, biodegradability, and encapsulation capability[4] among other candidates such as nanoparticles,[5] polymers,[6] and lipids.[7]

In particular, DNA has emerged as a promising building block in the development of hydrogels for molecular carriers due to its versatile functionality and programmability.[8−10] The base sequences within the DNA hydrogel can be strategically designed so as to allow the selective loading of cargo molecules with sequence-dictated interactions such as hybridization,[11] motifs,[12] and aptamers.[13,14] In addition to its sequence-specific loading, DNA can load cargo molecules through various binding modes, including groove binding[15] and intercalation.[16,17] Moreover, DNA hydrogels can be engineered into stimuli-responsive materials capable of shape memory,[18] volume expansion,[19,20] and condensation,[21−23] making them useful for targeted release of cargo. However, the susceptibility of DNA to nuclease has posed the vulnerability of DNA hydrogels in the application of molecular delivery.[24,25] The in vivo presence of nuclease leads to the degradation of the DNA hydrogel, hindering the protection and selective release of cargo molecules.

Electrostatic interactions are potentially crucial for exploiting the advantages of and addressing the challenges associated with DNA hydrogels. DNA, being a highly negative polyelectrolyte due to its phosphate backbone, undergoes the phase changes upon the addition of polycations such as spermidine, spermine, and poly-L-lysine, while maintaining base-pairing interactions.[26,27] The state of DNA−polycation complexes can be further modulated by monovalent cations, which disrupt these complex interactions.[28,29] Furthermore, DNA−polyamine complexes have been observed to protect DNA from nuclease degradation due to either conformational changes in the DNA or limited enzyme access to recognition sites.[30] Meanwhile, the complexation of DNA with polyamine, such as spermine, has demonstrated efficacy in gene delivery applications and exhibited biocompatibility.[31−33] Whereas the utilization of polycations to induce shape changes in DNA hydrogels has been acknowledged,[21,34,35] the processes of condensation,

Received: November 24, 2023
Revised: April 19, 2024
Accepted: April 28, 2024
Published: May 2, 2024

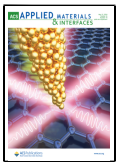

https://doi.org/10.1021/acsami.3c17633
ACS Appl. Mater. Interfaces 2024, 16, 24162−24171

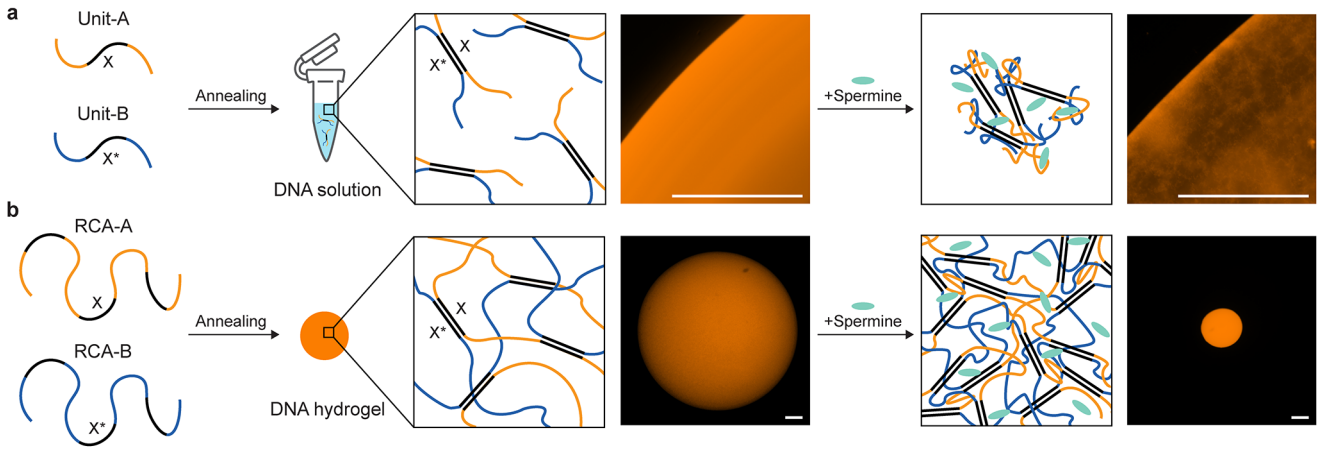

Figure 1. Comparison between phase separation of dissolved DNA and volume change of gelated DNA after adding spermine. (a) Formation of solid aggregates from a DNA solution consisting of annealed repeating units of RCA (72 nt each) with 12 bp cross-link region, denoted as X and X*, upon addition of spermine. (b) Reduction of the entire volume of pure DNA hydrogel, which is fabricated by annealing long RCA strands containing repeated 12 bp cross-link regions denoted as X and X*, in the presence of spermine. Scale bars: 200 μm.

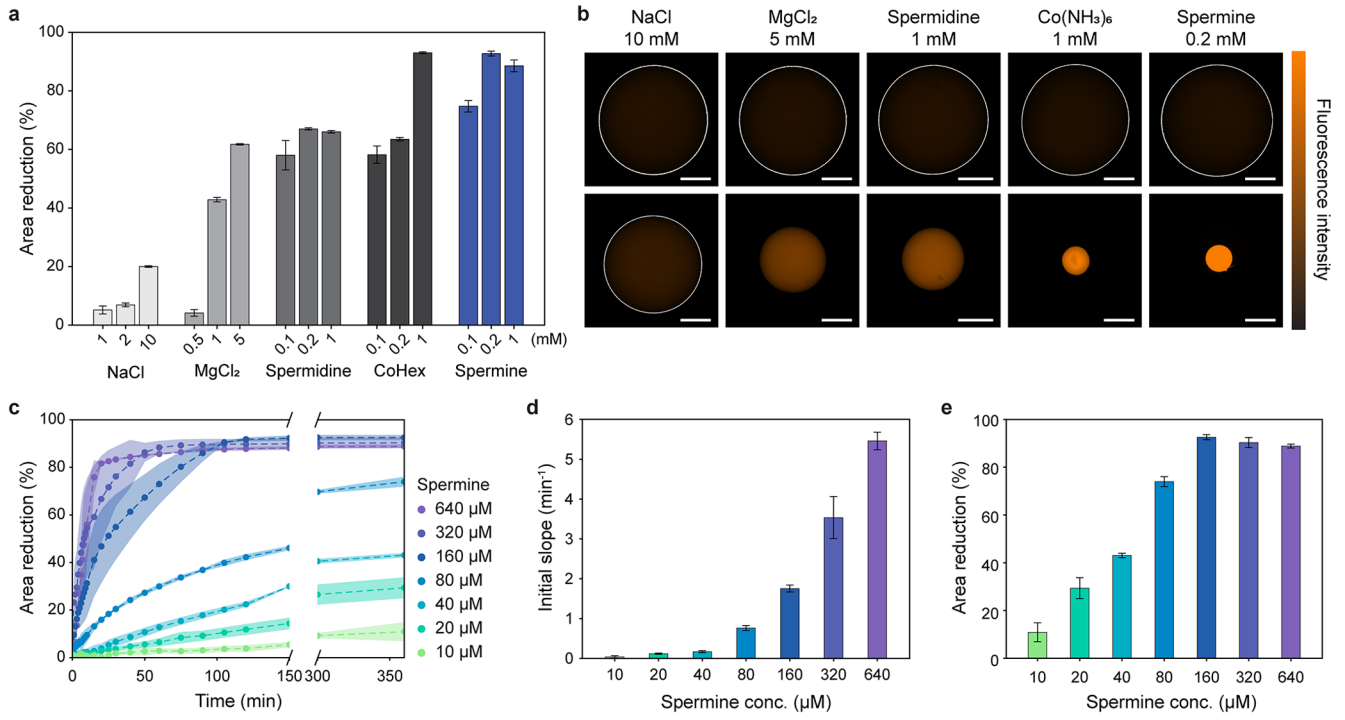

Figure 2. Ion-dependent volumetric condensation of RCA hydrogel. (a) Percentage area reduction ($[1 - A_t/A_0] \times 100$) after incubating for 24 h with various concentrations of mono- and multivalent cations, including Na(+), Mg(2+), spermidine(3+), cobalt hexammine(3+), and spermine(4+). Error bars: SDs (n = 4). (b) Top: fluorescence images of hydrogels in their initial states in 1X TE/10 mM NaCl buffer. Bottom: final states of hydrogels with the addition of the most effective concentration for each cation. (c) Time-dependent condensation profile of hydrogels with various concentrations of spermine, calculated by the percentage area reduction at each time point. Shaded area: SDs ($n \geq 3$). (d) Initial slope of condensation results shown in (c), obtained using the curve_fit function in scipy with a linear function. Error bars: SDs computed by the covariance of the optimal slope value. (e) Percentage area reduction after incubating for 360 min with various concentrations of spermine. Error bar: SDs. Scale bars: (b) 500 μm.

expansion, and degradation within these hydrogels as a molecular carrier remain largely unexplored.

Here, we develop a simple way of controlling the enzyme resistance of DNA hydrogels using cation-mediated condensation and expansion. Pure DNA hydrogels were first prepared by hybridizing long DNA single strands containing repetitive sequences obtained through the rolling circle amplification (RCA) (Figure S1).[36,37] Then, tetravalent spermine was employed to condense these DNA hydrogels using its strong electrostatic interaction with DNA backbones, making them nondegradable by DNase I to protect cargo molecules inside. We could make them degradable again for cargo release by adding NaCl that expanded them to the original, uncondensed state by interfering with the DNA–spermine interaction. The effects of cation and salt conditions on the condensation, expansion, and degradation of DNA

https://doi.org/10.1021/acsami.3c17633
ACS Appl. Mater. Interfaces 2024, 16, 24162−24171

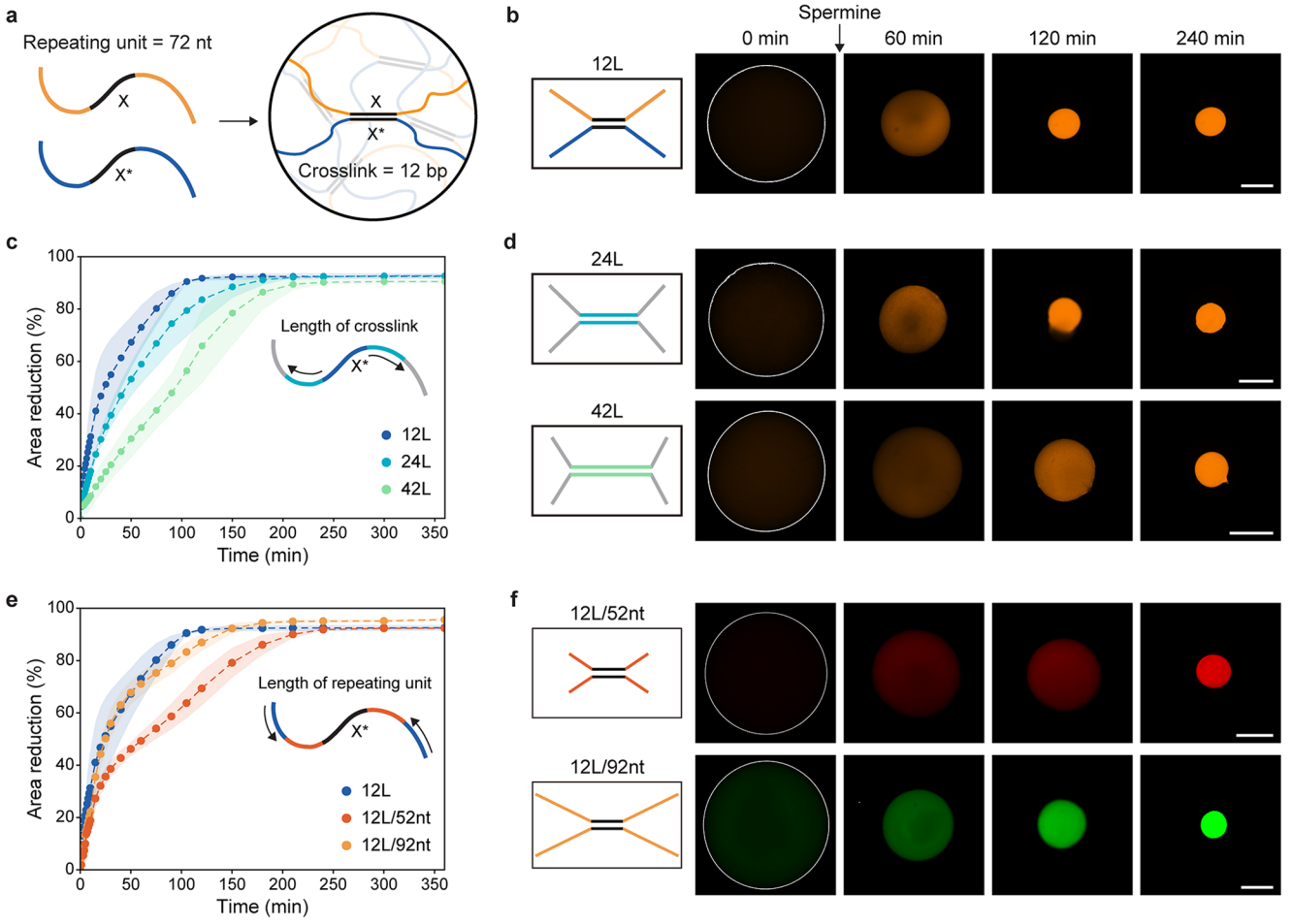

Figure 3. Influence of double-stranded to single-stranded ratio in network on hydrogel condensation. (a) Schematic representation of a default type of DNA hydrogel prepared by two RCA strands with 72 nt repeating unit and 12 bp cross-link region. (b) Fluorescence images of time-dependent condensation of 12L hydrogels. (c) Time-dependent condensation profile of hydrogels with different lengths of cross-link, calculated by the percentage area reduction at each time point. Shaded area, SDs ($n \geq 3$). (d) Fluorescence images of time-dependent condensation of 24L and 42L hydrogels. (e) Time-dependent condensation profile of hydrogels with different length of repeating unit, calculated by the percentage area reduction at each time point. Shaded area: SDs ($n \geq 3$). (f) Fluorescence images of time-dependent condensation of 12L/52nt and 12L/92nt hydrogels. Scale bars: 500 μm.

hydrogels were thoroughly investigated. We also explored a proof-of-concept application of DNA hydrogels as a molecular carrier by loading and releasing DAPI as a representative cargo molecule.

RESULTS AND DISCUSSION

Cation-Induced Hydrogel Condensation. DNA hydrogels were fabricated using two RCA strands (RCA-A and -B) consisting of 72 nt repeating units.[36] Within each unit, 12 nt complementary regions of two RCA strands, X and X*, could be hybridized, becoming the cross-linking point of the hydrogel. We prepared two 72 nt DNA single strands corresponding to a repeating unit of hydrogels (Figure 1a). When mixing these strands with spermine in solution, solid aggregates of DNA were formed throughout the solution via the phase separation phenomenon because the dsDNA portion induced a high electrostatic interaction between DNA and spermine.[26,28] In the hydrogel, a similar interaction between spermine and DNA led to a drastic reduction in the volume of the hydrogel (Figure 1b) due to the confinement of DNA chains as a network.

We first examined the condensation behavior of DNA hydrogels with different types of cations. Before condensation, other ions in DNA hydrogels should be expelled to inspect the condensation aspect caused by the target cation. However, hydrogels could not maintain their shape and structure when washed with 1X TE buffer (Figure S2). The 12 bp long DNA cross-links might become electrostatically unstable without cations due to their low binding energy and the high density of negative charges within hydrogels. Therefore, we rinsed the hydrogels with 1X TE buffer containing 10 mM NaCl to maintain stability after eliminating the excess ions for the subsequent experiments.

Tri- and tetravalent cations such as spermidine(3+), cobalt hexammine(3+), and spermine(4+) induced an effective volumetric condensation up to ~92% of area reduction at relatively low concentrations compared to mono- and divalent ones (Figures 2a and 2b). It might be because the cations whose valence was higher than three could induce liquid−liquid phase separation of DNA through their binding to DNA grooves and backbones.[38] Cobalt hexammine was shown to be more efficient in condensing the hydrogel than spermidine while they have the same valence.[39] Nonetheless, if we used

https://doi.org/10.1021/acsami.3c17633
ACS Appl. Mater. Interfaces 2024, 16, 24162−24171

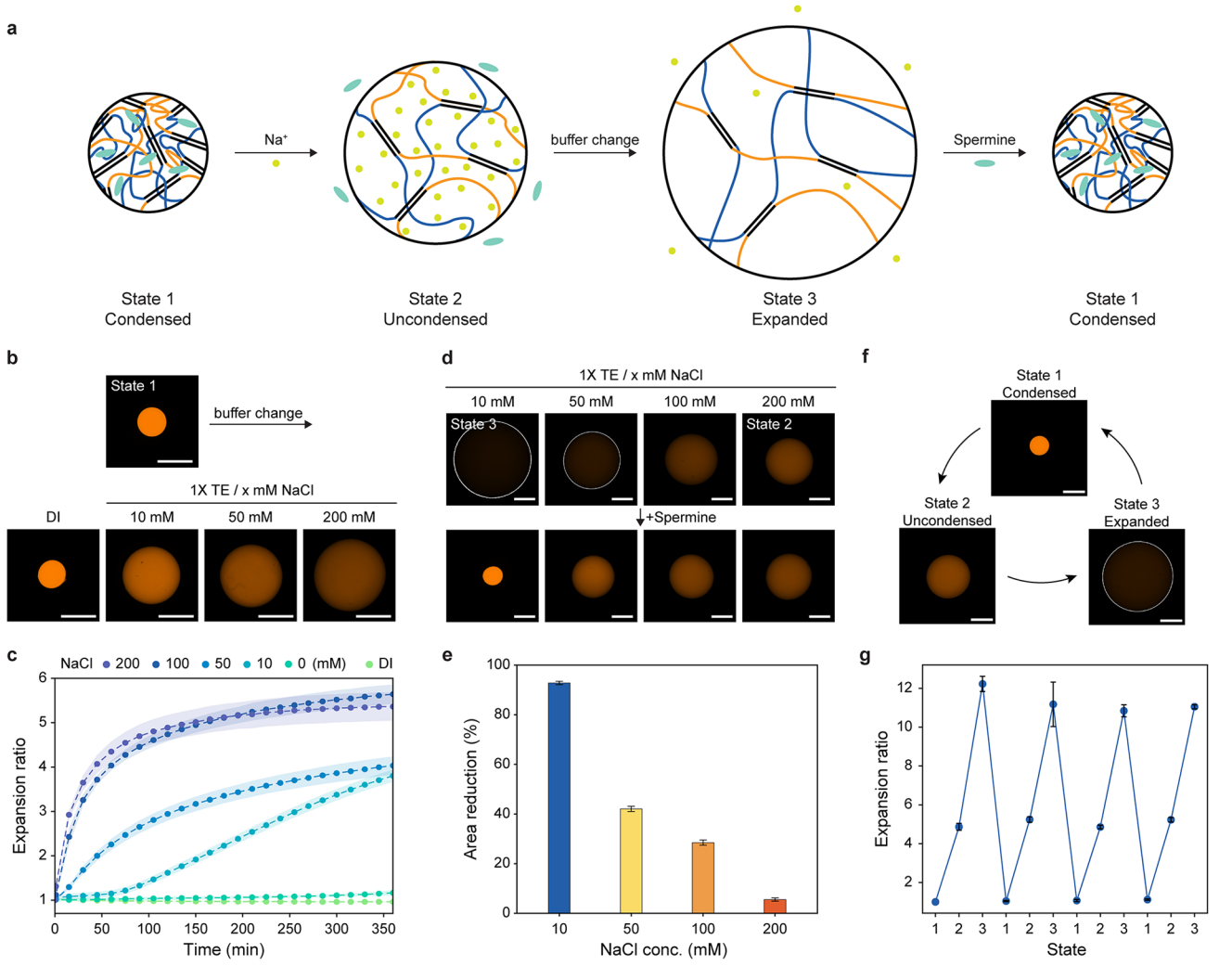

Figure 4. Effect of salt in the condensation and expansion of hydrogels. (a) Schematic illustrations of repetitive condensation and expansion of hydrogels with surrounding ion circumstances. (b) Process of going from state 1 (condensed with spermine) to state 2 (uncondensed) with varying NaCl concentrations. Stated the conditions of the changed buffer. (c) Time-dependent expansion profile of condensed hydrogels with DI water and different NaCl concentrations in 1X TE, calculated by the expansion ratio (A_t/A_0) at each time point. (d) Spermine-induced condensation with the varying NaCl concentrations in 1X TE buffer. Stated the equilibrated conditions of the initial buffer. (e) Percentage area reduction after 24 h of hydrogel incubation with spermine in TE/NaCl buffer. Error bar: SDs (n = 4). (f) Repetitive hydrogel condensation and expansion controlled by the ion conditions. State 1: spermine-induced condensation. State 2: salt-induced uncondensed condition; State 3: fully expanded by excluding the excess NaCl. (g) Four repeating cycles of hydrogel volume changes. Error bar: SDs (n = 4). Scale bars: (b, d, f) 500 μm.

more than ten times higher concentrations of Na(+) and Mg(2+), the volume of hydrogels was reduced up to ~82% because they could effectively screen the electrostatic repulsion of negatively charged phosphate backbones (Figure S3).

We selected spermine as a representative cation to further investigate the characteristics of hydrogel condensation by varying its concentration, as it turned out to be the most efficient condensing agent among the cations we tested (Figure 2a). The condensation process was significantly accelerated with the concentration of spermine, as the diffusive flux of spermine molecules would be proportional to the concentration gradient (Figures 2c and 2d). It was quickly saturated approximately in 20 min when 640 μM of spermine was used. Interestingly, the area reduction was not monotonically increased with the spermine concentration, and its maximum value (~92%) appeared at 160 μM of spermine (Figure 2e). This observation is in complete accord with the previous findings on the resolubilization of DNA aggregates under higher concentrations of polyvalent cations.[40,41] Concentrations beyond this critical threshold became less effective in hydrogel condensation. Upon exceeding the concentration of 640 μM, highly inhomogeneous and irregular condensations occurred (Figure S4).

Effect of the Cross-Linking Ratio on Condensation. The network structure of hydrogels plays a critical role in determining their physical properties.[42] Within a default 72 nt length repeating unit and 12 bp cross-link hydrogel (Figure 3a), we controlled the ratio of dsDNA to ssDNA by manipulating the length of the cross-link between two DNA single strands. The sequence of the RCA-B strand was varied to be hybridized with the RCA-A strand at various lengths of 12, 24, and 42 bps, labeled as 12L, 24L, and 42L, respectively. Once made, these hydrogels were condensed using the same concentration of spermine (160 μM), and their condensation behavior was analyzed (Figure 3b–d). Notably, increasing the cross-linking ratio (from 12/72 to 42/72) slowed the

https://doi.org/10.1021/acsami.3c17633
ACS Appl. Mater. Interfaces 2024, 16, 24162−24171

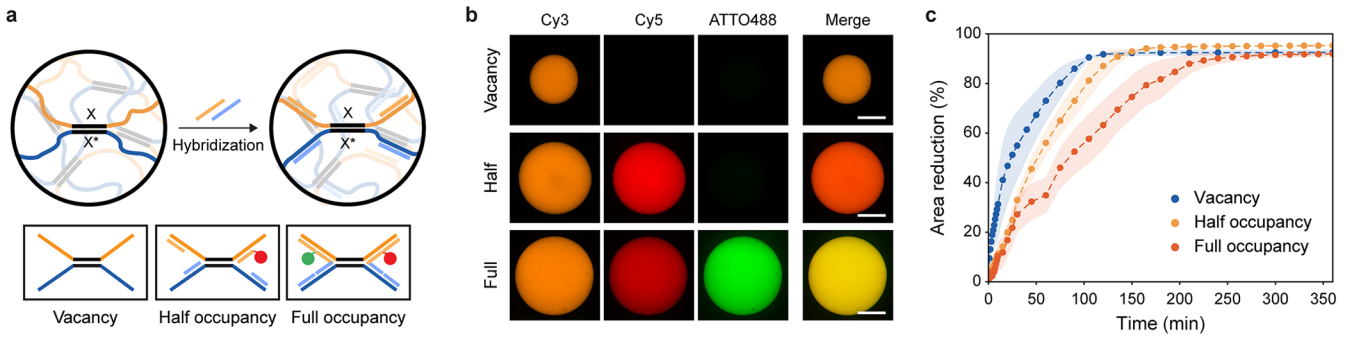

Figure 5. Cargo loading into the hydrogel and their condensation behaviors. (a) Schematic representation of loading cargo strands into the vacancies of the 12L hydrogel, named the hybridization ratio among total vacancy and the number of additional strands for each RCA strands. Some cargo strands were modified with fluorophore including Cy5 and ATTO488. (b) Fluorescence images to validate the adequate loading of cargo strands comparing pristine 12L hydrogel, hydrogel with half cargo, and hydrogel with full cargo. (c) Time-dependent condensation profile of hydrogels with various cargo strands, calculated by the percentage area reduction at each time point. Shaded area: SDs ($n \geq 3$). Scale bars: (b) 500 μm.

condensation, whereas it did not affect the final level of the area reduction (Figure 3c). Hence, the cross-linking ratio would be an important design variable to independently control the condensation speed without affecting the level of the area reduction. Scanning electron micrograph (SEM) images of freeze-dried samples revealed that the network packing of condensed hydrogels was also affected by the condensation speed. Although the microstructures before condensation were observed to be comparable between samples, hydrogels with a lowercross-linking ratio displayed smaller pores (Figure S5).

Similar results were obtained when we tuned the cross-linking ratio by altering the unit length of two RCA strands from 72 nt to 52 and 92 nt while keeping the length of the cross-link to 12 bp denoted as 12L/52nt and 12L/92nt, respectively (Figure 3b,e,f). The condensation speed was reduced for 12L/52nt as the cross-linking ratio was increased from 12/72 to 12/52 while the final area reduction remained at a similar level. However, the condensation speed of 12L/92nt hardly changed, suggesting that it was saturated already when the 72 nt repeating unit was used (Figure 3e).

Reversible and Repeatable Volume Change. Salt ions affect the phase separation behavior of DNA by interrupting the interaction between spermine and DNA due to its smaller molecular size than polyamine, which is a common phenomenon for polyelectrolyte complexes.[29,43] Indeed, DNA solid aggregates formed by spermine gradually dissolved with increasing NaCl concentrations for both the unit and RCA strands (Figure S6). We employed this phenomenon to make DNA hydrogels change their volume reversibly and repeatedly through three representative states: condensed state by spermine (state 1), uncondensed state by sodium ions (state 2), and fully expanded state by rinsing the excess sodium ions (state 3) (Figure 4a).

DNA hydrogels initially condensed with 160 μM of spermine were immersed in TE buffers supplemented with various concentrations of NaCl to observe its expansion behavior, from state 1 to state 2 (Figure 4b,c). As the concentration of supplement NaCl increased, condensed hydrogels expanded faster and larger. The expansion ratio of hydrogels submerged in buffers with more than 100 mM NaCl expanded at around 80% within the first hour and fully converged in 6 h, while it took 48 h for hydrogels in other buffers (Figure S7). It should be noted that the condensed hydrogels soaked in distilled water barely expanded (Figures 4c and S7). This is because spermine ions not only screen the negative charge in the phosphate backbone of DNA but also strongly bind to the groove and backbone during condensation.[38] Accordingly, the interactions are stably maintained, unless interrupted by smaller cations.

While DNA hydrogels can expand effectively with the addition of NaCl at a sufficiently high concentration, these expanded hydrogels cannot be condensed again by adding more spermine directly. It is because sodium ions more preferentially bind DNA and screen the electrostatic interaction, hindering the interaction between spermine and DNA. To demonstrate, DNA hydrogels were equilibrated in TE buffers supplemented with various concentrations of NaCl before being condensed by spermine (Figure 4d). Since the monovalent cations bound the phosphate backbone and screened the electrostatic repulsion between DNA, the volume of hydrogels in equilibrium decreased with the concentration of NaCl in the immersed buffer. When 160 μM spermine was added, condensation became significantly ineffective except for the 10 mM NaCl case (Figure 4e). Hence, a dilution step from state 2 to state 3 is necessary to reactivate the spermine-mediated condensation of DNA hydrogels expanded with NaCl.

Based on these observations, we designed an experimental process for repetitive expansion and condensation of DNA hydrogels (Figure 4f). The condensed state of hydrogels using spermine (state 1) could be moderately expanded by introducing salt and become uncondensed (state 2), and then, the excess salt was removed by buffer exchange to fully expand them (state 3). The hydrogels could repeatedly react to spermine and efficiently condense after undergoing the aforementioned steps. For repeating cycles of condensation and expansion, DNA hydrogels could robustly sustain their spherical configurations and exhibit consistent levels of expansion ratios approximately 5 for state 2 and 10−12 for state 3 (Figures 4g and S8).

Cargo Strand Loading. One of the most notable advantages of DNA hydrogels is that cargo molecules can be readily and selectively loaded into the hydrogel through the hybridization of complementary strands[36,44] and the intercalation of binding molecules.[45] Here, we investigated the loading of complementary strands into DNA hydrogels and their effect on spermine-mediated condensation. The cargo

https://doi.org/10.1021/acsami.3c17633
ACS Appl. Mater. Interfaces 2024, 16, 24162−24171

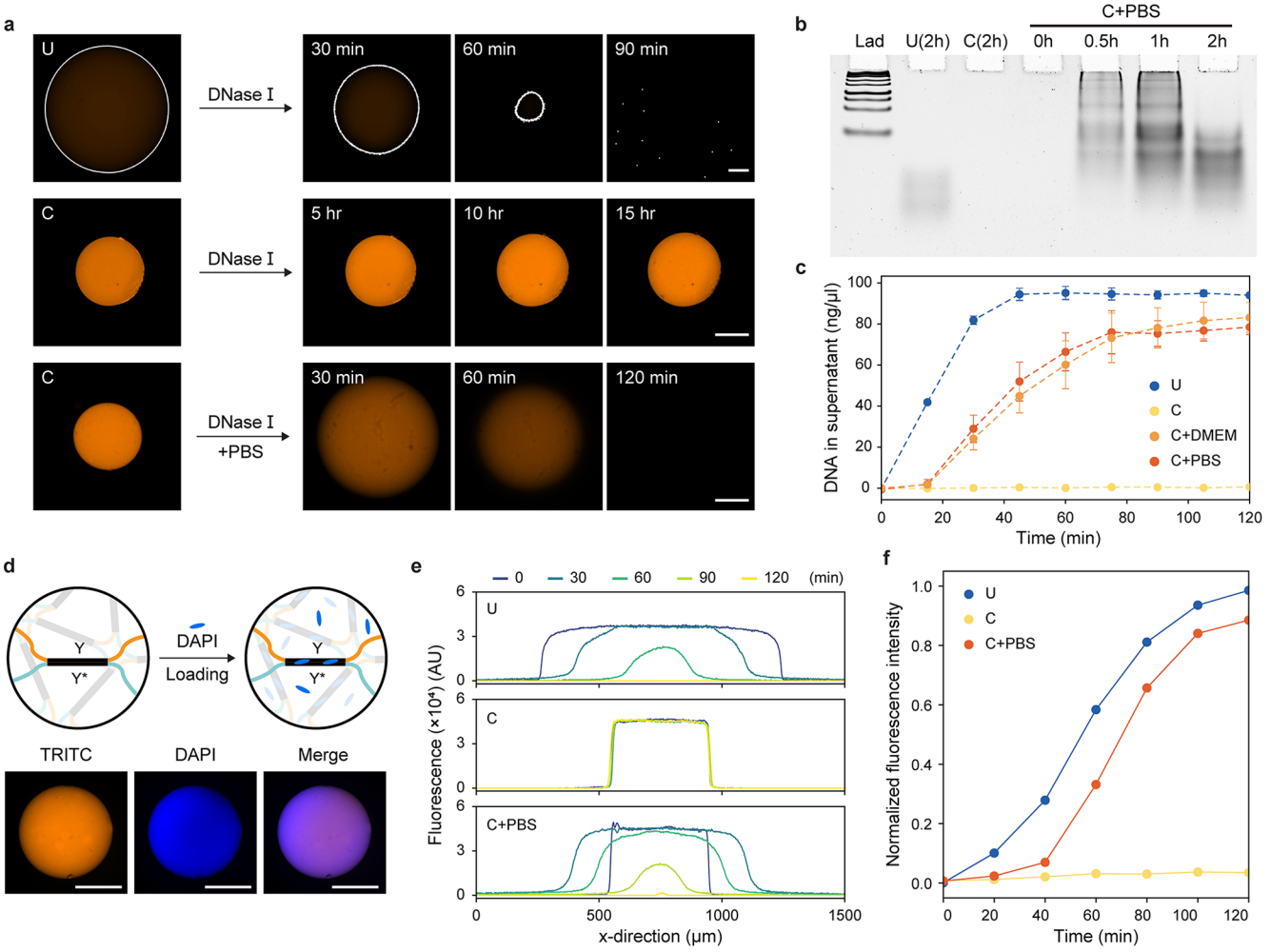

Figure 6. Controlled enzyme resistance of condensed hydrogels for drug delivery applications. (a) Enzymatic degradation of DNA hydrogel of different states and condition. Top: uncondensed hydrogel in normal DNase I solution (U). Middle: condensed hydrogel in normal DNase I solution (C). Bottom: condensed hydrogel in DNase I solution supplemented with 1X PBS(C+PBS). (b) PAGE result of supernatant of U and C after 2 h and C+PBS during 2 h. Ladder: GeneRuler Low Range DNA Ladder (Thermo Scientific). (c) DNA concentrations in supernatant during degradation of U, C, C+PBS, and C+DMEM (condensed hydrogel in DNase I solution supplemented with DMEM). (d) Schematic illustration of DAPI binding at dsDNA part in 42L hydrogel and fluorescence images to validate the adequate loading of DAPI. (e) Line segment analysis in DAPI channel of U, C, and C+PBS during 2 h. (f) Normalized fluorescence intensity of DAPI (excitation 350 nm/emission 470 nm) in supernatant during degradation of U, C, and C+PBS. Scale bars: (a) 200 μm and (d) 500 μm.

strands were designed to be complementary to specific single-stranded regions of the 12L hydrogel that have the most vacancies in the backbone and were either half or fully occupied (Figure 5a). To verify the successful embedment of these cargo strands into the hydrogel, Cy5 and ATTO488 fluorophores were attached to them (Figure 5b).

Cargo-laden hydrogels were condensed to a similar level (the area reduction ratio of ~0.92) compared to hydrogels without cargo; however, the cargo strands slowed the condensation (Figure 5c). As more strands were loaded, the condensation became slower as the double-stranded portion increased with cargos. The final area reduction remained unaffected by the presence of cargo strands even in the case of full occupancy where the entire hydrogel network was formed with double strands. It is interesting how hybridizing cargo strands affected the condensation speed. For example, in half occupancy of cargo strands, the gathered hybridization where double strands were formed continuously slowed the condensation speed more than the dispersed hybridization where the formation of double strands was discrete (Figure S9).

Enzyme Resistance of Condensed DNA Hydrogels. For DNA hydrogels to be used as an effective molecular carrier, it is important to control their degradation in solution environment crucial for both protection and release of cargo.[3] It has been reported that the condensation of DNA facilitated by polyamines can effectively protect the DNA from enzymatic degradation, either through conformational changes of DNA substrates or by limited accessibility of the recognition sites for the enzyme.[30] Here, we showcase the enzyme resistance and retarded degradation of the condensed DNA hydrogels.

We first probed the enzyme reactivity of our DNA hydrogels by incubating uncondensed hydrogels with DNase I at different concentrations (Figures 6a, 6b, and S10). Since DNase I is an endonuclease that can cleave any type of DNA, these hydrogels were gradually degraded and culminated in complete dissolution at DNase I concentrations exceeding 20 U/mL. On the contrary, condensed hydrogels exhibited an

https://doi.org/10.1021/acsami.3c17633
ACS Appl. Mater. Interfaces 2024, 16, 24162−24171

unnoticeable response to the enzyme, preserving their structural integrity even after being incubated for 50 days (Figures 6a, 6b, and S11). However, if the condensed DNA hydrogels were submerged in 1X TE buffer supplemented with salt, their degradation was observed to be delayed depending on the concentrations of the salt (Figure S12). The onset of degradation coincided with the salt-induced expansion ratio reaching approximately 2.5 (Figure 4c), followed by a gradual degradation by DNase I. Specifically, at salt concentrations over 100 mM, degradation commenced after ∼30 min due to the expansion ratio reaching ∼2.5. At 50 mM, it began after ∼75 min, while at 10 mM, no decomposition was observed within the experimental time frame. Similarly, when our DNA hydrogels were immersed with DNase I in physiological buffers containing NaCl such as PBS (phosphate buffered saline) and DMEM (Dulbecco modified eagle medium), they resulted in the initial expansion and the subsequent degradation (Figures 6a and 6b). The degradation prevailed over the expansion in ∼30 min according to the size and concentration of DNA fragments measured in the supernatant of the solution (Figures 6b and 6c). Furthermore, we also investigated the impact of FBS (fetal bovine serum) which contains various nucleases[46] on hydrogel stability (Figure S13). As a control group, uncondensed hydrogels exposed to FBS alone exhibited slight degradation over 2 h due to the inherent nucleases in the solution. In contrast, when FBS was supplemented with DNase I, uncondensed hydrogels were immediately degraded. The degradation of condensed hydrogels in the same solution was delayed, as in the previous results in PBS and DMEM.

Moreover, we considered the variation in cation compositions across different body fluid compartments, classified into two major components as intracellular and extracellular fluids. A significant distinction between the fluids is observed in the concentrations of monovalent cations, particularly Na^+ and K^+.[47] With regard to this, the analysis of DNA hydrogel degradation in buffers with varying K^+ concentrations revealed a similar trend of slowed degradation, comparable to the Na^+ supplementing buffer (Figure S14).

To demonstrate the usefulness of our hydrogel system as a molecular carrier, we loaded DAPI as a model molecular cargo into the hydrogel. DAPI, a minor groove binder known for its significant DNA binding capability and fluorescence properties, is widely utilized as a staining dye selectively binding to double-stranded DNA. Unlike nucleic acid cargo, DNA binding molecules like DAPI have greater affinity for hydrogels with larger double-stranded portions, such as the 42L hydrogel. To confirm these, we loaded an equal amount of DAPI into 12L, 24L, and 42L hydrogel and monitored the release kinetics to compare the loading capacity between them. The results suggested that the 42L hydrogel released the largest amount of DAPI, as indicated by the highest fluorescence intensity over 2 h (Figure S15).

Accordingly, we selected 42L hydrogels to ensure a sufficient amount of DAPI loading, as confirmed by fluorescence images (Figure 6d). Subsequent DAPI release kinetics were assessed by quantifying fluorescence intensities extracted from sequential imaging at specific time points (Figures 6f and S16). Uncondensed hydrogels in a normal DNase I solution underwent gradual degradation from the outer side, while condensed hydrogels in the same solution retained their shape and DAPI fluorescence. In the presence of salt in the solution, however, condensed hydrogels first expanded while preserving their fluorescence level and then manifested degradation-mediated DAPI release.

DAPI release kinetics was also examined by monitoring fluorescence intensities in the supernatant over time without agitation (Figure 6f). The overall tendency of DAPI release was consistent with that of DNA fragments analysis in the supernatant. The uncondensed hydrogel showed early release of DAPI, whereas the condensed hydrogel exhibited no release. In contrast, the condensed hydrogel incubated in a PBS-supplemented DNase I solution demonstrated a delayed release of DAPI.

In addition, we loaded doxorubicin (DOX), a renowned DNA intercalator, onto the 42L hydrogel to validate the suitability of our molecular carrier for different types of binding molecules. The release kinetics of DOX were investigated by using the same methodology as that for DAPI (Figure S17). The intercalated cargo in the uncondensed hydrogel was release at an early stage, while that in condensed hydrogel exhibited no release. Conversely, the intercalator within the condensed hydrogel, in an environment with salt, was released at a later stage.

CONCLUSION

Molecular carriers require various functionalities including stimuli-responsive shape and property changes and programmable biodegradation to accomplish an effective delivery to a target.[1,2] In this study, we proposed an effective way of controlling the condensation, expansion, and degradation of DNA hydrogels by cations and systematically analyzed these properties. Interactions between DNA and spermine employed in the proposed method enabled us to achieve a drastically fast and extensive volume condensation of DNA hydrogels compared to conventional approaches using toehold-mediated strand displacement and various DNA motifs.[19,23] The condensation speed could be independently modulated by designing the cross-linking ratio of constituent DNA strands while maintaining the level of condensation. Upon adding excess NaCl, the condensed hydrogels could revert to their original configuration due to the interference of salt ions in the binding of spermine and DNA backbones.

Remarkably, our DNA hydrogels exhibited strong enzymatic resistance when condensed unlike typical ones vulnerable to nuclease degradation.[30] The resistant property could disappear after expansion, shown to be useful for modulating degradation behavior. We showcased proof-of-concept application of DNA hydrogels as a molecular carrier using DAPI as a representative cargo. We could observe a gradual release of DAPI mediated by the degradation of cargo-loaded condensed DNA hydrogels in physiological buffers. While further exploration is needed to assess its efficacy with various cargo molecules and to investigate its performance in vivo across a wide range of sizes, the proposed method is expected to offer a versatile way of developing DNA hydrogels for molecular carriers with tunable degradation properties that are important to protecting and releasing cargo molecules.

EXPERIMENTAL SECTION

Materials. All DNA strands were purchased from Integrated DNA Technologies Inc. and are listed in Table S1. Chemicals such as 5 M NaCl (S5150), spermidine (05292), spermine (S1141), cobalt hexammine (H7891), 100X TE buffer (T9285), DAPI (MBD0015), and doxorubicin hydrochloride (44583) were purchased from Sigma-Aldrich. T4 ligase (E-3061) and 1 M $MgCl_2$ (C-9022) were

https://doi.org/10.1021/acsami.3c17633
ACS Appl. Mater. Interfaces 2024, 16, 24162−24171

purchased from Bioneer, and DNase I (M0303S) was purchased from New England Biolabs. Other chemicals and enzymes such as 10X PBS (AM9624), DNTP mix (R1121), DMEM (11995065), Exonuclease 1(EN0582), Exonuclease 3(EN0191), Φ29 polymerase (EP0094), and inorganic pyrophosphatase (EF0021) were purchased from Thermo Fisher.

Phase Separation of Unit DNA Strands. The unit DNA 2X solution was prepared with two strands of DNA having the same sequences as the repeating unit. The final phosphate concentration of the solution was 2 mM in a 1X TE buffer containing 10 mM NaCl. Then, the solution was annealed as heating to 85 °C, keeping 5 min, and lowering the temperature from 85 to 25 °C at a rate of −1 °C/min. The spermine 2X solution was prepared with the final amine concentration of 2 mM in the same buffer condition. After the two solutions thoroughly mixed in a 1:1 volume ratio by pipetting, the mixed solution was mounted on the confocal dish and incubated at RT for 10 min. The final phase separation images were obtained under a 10× or 40× fluorescence microscope.

Rolling Circle Amplification and Hydrogel Fabrication. Rolling circle amplification (RCA) was performed according to the previously reported method,[36,48] and the graphical abstract for the process is in the SI figure. After rinsing with TE buffer, the RCA product was diluted to 0.5 g L^{-1} and homogenized by heating to 85 °C for 5 min, rigorous vortexing, and incubating at RT overnight. The uniformly dissolved RCA product was spun down 15000*g* for 10 min with a 30 kDa cutoff Amicon filter (Merck Millipore) to acquire a concentrated stock solution. The concentrations of solutions were measured using a NanoDrop spectrophotometer (Thermo Fisher Scientific, USA).

The precursor solution was prepared by mixing RCA product A and B stock solutions in a 1:1 stoichiometric proportion, as the final concentration is 5 g L^{-1} A and B each in 1X TE buffer containing 200 mM NaCl. To fabricate a spherical hydrogel, 200 μL of mineral oil was filled in an *x* mm diameter well, and a 1 μL droplet of the precursor solution was injected. Then, the entire well was heated to 85 °C for 5 min on a hot plate and cooled to RT. The hydrogels were washed with 1X TE buffer containing 200 mM NaCl and stored at 4 °C.

Hydrogel Buffer Exchange and Ion-Induced Condensation. Before investigating hydrogel condensation by cations, the hydrogels were washed with 1X TE buffer containing 10 mM NaCl to remove excess salt from the hydrogel. Each hydrogel was placed in 500 μL of washing buffer in a well of μ-Slide 8 well (ibidi, 80821), and the buffer was freshly exchanged three times every 20 min. The salt-containing buffer was utilized to maintain stability because the hydrogel rapidly collapsed in the absence of salt due to dissociation of the dsDNA linker.

To condense and observe the hydrogel, 5 μL of 100X cation solution was added to the well where the expanded hydrogel was immersed in 500 μL of washing buffer. Immediately after mixing by pipetting, the condensation of the hydrogel was examined as a time lapse through a fluorescence microscope. The hydrogel images were extracted from each time frame, and the number of pixels in the 2D projection image was analyzed by using Python to compare the initial uncondensed state.

Fluorescence Microscopy Measurements. Hydrogel images were obtained with a Nikon Ti2-E microscope equipped with a 2X Apo objective, and fluorescence images were obtained with Nikon fluorescence filters depending on the type of fluorophore used. In addition, 100% humidity and RT temperature were set with an incubator (Nikon, Japan) to prevent evaporation of the buffer containing the hydrogel during time-lapse imaging. Phase separation images were obtained with a 40× Apo objective.

Enzymatic Responsiveness of the Hydrogel. Hydrogel samples were placed in 100 μL of DNase I solution in a tube or 8-well slide. The tube or slide was placed in an adequate incubator, and the temperature was set to 37 °C, the optimal working temperature of DNase I. The degradation behavior of the hydrogel was identified in two ways. In the case of fluorescence images, the degradation was observed by time-lapse imaging without additional mixing, while in the case of measuring the DNA concentration of the supernatant in the tube, the supernatant was extracted after careful mixing by pipetting. The DNA concentration in the supernatant was measured with NanoDrop every 15 min.

■ ASSOCIATED CONTENT

Supporting Information

The Supporting Information is available free of charge at https://pubs.acs.org/doi/10.1021/acsami.3c17633.

Single-stranded DNA production via rolling circle amplification (RCA), instability of the hydrogel depending on washing buffer, condensation with the high concentrations of NaCl and $MgCl_2$, condensation with high concentration of spermine (1280 μM), SEM images of the hydrogels controlling the hybridization length, dissolution of the phase-separated solid aggregate by adding NaCl, time-dependent expansion of condensed hydrogels for 48 h, fluorescence images of repetitive condensation and expansion, cargo loading into the hydrogel and their condensation behaviors, degradation of uncondensed 12L hydrogel, enzyme resistance of condensed hydrogels after 50 days, degradation of condensed 12L hydrogel with varying NaCl concentration, degradation of condensed 12L hydrogel incubating with FBS (Fetal Bovine Serum), degradation of condensed 12L hydrogel with varying KCl concentrations, normalized fluorescence intensity of DAPI in supernatant during degradation with varying linker length of hydrogel, fluorescence images of the degradation of DAPI-loaded hydrogel, normalized fluorescence intensity of doxorubicin in supernatant during degradation of U, C, and C+PBS, DNA sequences and the modification code for ordering at IDT (PDF)

■ AUTHOR INFORMATION

Corresponding Author

Do-Nyun Kim − *Department of Mechanical Engineering, Seoul National University, Seoul 08826, Korea; Institute of Advanced Machines and Design and Institute of Engineering Research, Seoul National University, Seoul 08826, Korea;* orcid.org/0000-0003-0896-4552; Email: dnkim@snu.ac.kr

Authors

Kyounghwa Jeon − *Department of Mechanical Engineering, Seoul National University, Seoul 08826, Korea;* orcid.org/0000-0003-2020-9736

Chanseok Lee − *Institute of Advanced Machines and Design, Seoul National University, Seoul 08826, Korea;* Present Address: Department of Bionano Engineering, Hanyang University, Ansan 15588, Korea; orcid.org/0000-0002-7969-4345

Jae Young Lee − *Institute of Advanced Machines and Design, Seoul National University, Seoul 08826, Korea;* orcid.org/0000-0002-6438-2699

Complete contact information is available at: https://pubs.acs.org/10.1021/acsami.3c17633

Author Contributions

D.-N.K., C.L., and K.J. conceptualized the idea and conceived the methodology. K.J. investigated and validated the concept.

https://doi.org/10.1021/acsami.3c17633
ACS Appl. Mater. Interfaces 2024, 16, 24162−24171

K.J., C.L., and J.Y.L. analyzed and visualized the data. D.-N.K. and K.J. wrote the original draft and reviewed and edited it.

Funding

This research was supported by the National Convergence Research of Scientific Challenges through the National Research Foundation of Korea (NRF) funded by the Ministry of Science and ICT (MSIT) [NRF-2020M3F7A1094299] and the Bio & Medical Technology Development Program through the National Research Foundation (NRF) funded by the Ministry of Science and ICT (MSIT) [NRF-2022M3E5F1018465].

Notes

The authors declare no competing financial interest.

REFERENCES

(1) Mitchell, M. J.; Billingsley, M. M.; Haley, R. M.; Wechsler, M. E.; Peppas, N. A.; Langer, R. Engineering Precision Nanoparticles for Drug Delivery. *Nat. Rev. Drug Discov* **2021**, *20*, 101−124.

(2) Li, J. Y.; Mooney, D. J. Designing Hydrogels for Controlled Drug Delivery. *Nat. Rev. Mater.* **2016**, *1*, 1−17.

(3) van den Berg, A. I. S.; Yun, C. O.; Schiffelers, R. M.; Hennink, W. E. Polymeric Delivery Systems for Nucleic Acid Therapeutics: Approaching the Clinic. *J. Controlled Release* **2021**, *331*, 121−141.

(4) Mo, F. L.; Jiang, K.; Zhao, D.; Wang, Y. Q.; Song, J.; Tan, W. H. DNA Hydrogel-Based Gene Editing and Drug Delivery Systems. *Adv. Drug Deliver Rev.* **2021**, *168*, 79−98.

(5) Manzano, M.; Vallet-Regí, M. Mesoporous Silica Nanoparticles for Drug Delivery. *Adv. Funct. Mater.* **2020**, *30*, 1902634.

(6) Thambi, T.; Deepagan, V. G.; Yoon, H. Y.; Han, H. S.; Kim, S. H.; Son, S.; Jo, D. G.; Ahn, C. H.; Suh, Y. D.; Kim, K.; Kim, K.; Kwon, I. C.; Lee, D. S.; Park, J. H. Hypoxia-Responsive Polymeric Nanoparticles for Tumor-Targeted Drug Delivery. *Biomaterials* **2014**, *35*, 1735−1743.

(7) Tenchov, R.; Bird, R.; Curtze, A. E.; Zhou, Q. Q. Lipid Nanoparticles-From Liposomes to mRNA Vaccine Delivery, a Landscape of Research Diversity and Advancement. *ACS Nano* **2021**, *15*, 16982−17015.

(8) Li, J.; Zheng, C.; Cansiz, S.; Wu, C. C.; Xu, J. H.; Cui, C.; Liu, Y.; Hou, W. J.; Wang, Y. Y.; Zhang, L. Q.; Teng, I. T.; Yang, H. H.; Tan, W. H. Self-assembly of DNA Nanohydrogels with Controllable Size and Stimuli-Responsive Property for Targeted Gene Regulation Therapy. *J. Am. Chem. Soc.* **2015**, *137*, 1412−1415.

(9) Zhang, L. B.; Jean, S. R.; Ahmed, S.; Aldridge, P. M.; Li, X. Y.; Fan, F. J.; Sargent, E. H.; Kelley, S. O. Multifunctional Quantum Dot DNA Hydrogels. *Nat. Commun.* **2017**, *8*, 381.

(10) Zhang, L.; Zhang, L. P.; Wang, Y. Q.; Jiang, K.; Gao, C.; Zhang, P. F.; Xie, Y. J.; Wang, B.; Zhao, Y.; Xiao, H. H.; Song, J. Regulating the Surface Topography of CpG Nanoadjuvants Coordination-driven Self-Assembly for Enhanced Tumor Immunotherapy. *Nanoscale Adv.* **2023**, *5*, 4758−4769.

(11) Han, S.; Park, Y.; Kim, H.; Nam, H.; Ko, O.; Lee, J. B. Double Controlled Release of Therapeutic RNA Modules through Injectable DNA-RNA Hybrid Hydrogel. *ACS Appl. Mater. Inter* **2020**, *12*, 55554−55563.

(12) Hu, Y. W.; Gao, S. J.; Lu, H. F.; Ying, J. Y. Acid-Resistant and Physiological pH-Responsive DNA Hydrogel Composed of A-Motif and i-Motif Toward Oral Insulin Delivery. *J. Am. Chem. Soc.* **2022**, *144*, 5461−5470.

(13) Song, P.; Ye, D.; Zuo, X.; Li, J.; Wang, J.; Liu, H.; Hwang, M. T.; Chao, J.; Su, S.; Wang, L.; Shi, J.; Wang, L.; Huang, W.; Lal, R.; Fan, C. DNA Hydrogel with Aptamer-Toehold-Based Recognition, Cloaking, and Decloaking of Circulating Tumor Cells for Live Cell Analysis. *Nano Lett.* **2017**, *17*, 5193−5198.

(14) Tang, J. P.; Jia, X. M.; Li, Q.; Cui, Z.; Liang, A. Q.; Ke, B.; Yang, D. Y.; Yao, C. A DNA-Based Hydrogel for Exosome Separation and Biomedical Applications. *P Natl. Acad. Sci. USA* **2023**, *120*, No. e2303822120.

(15) Liang, J. H.; Yang, X. S.; Li, C.; Zhang, B. B.; Liu, D. Q.; Fan, Y.; Hu, Y.; Du, J. Z. Injectable DNA Hydrogels with Intrinsic Antioxidant and Anti-Inflammatory Functions for Effectively Healing Bacteria-Infected Diabetic Wounds. *Chem. Mater.* **2023**, *35*, 9963−9977.

(16) Borum, R. M.; Moore, C.; Mantri, Y.; Xu, M.; Jokerst, J. V. Supramolecular Loading of DNA Hydrogels with Dye-Drug Conjugates for Real-Time Photoacoustic Monitoring of Chemotherapy. *Adv. Sci.* **2023**, *10*, 2204330.

(17) Zhang, L. P.; Wang, Y. Q.; Karges, J.; Tang, D. S.; Zhang, H. C.; Zou, K. X.; Song, J.; Xiao, H. H. Tetrahedral DNA Nanostructure with Interferon Stimulatory DNA Delivers Highly Potent Toxins and Activates the cGAS-STING Pathway for Robust Chemotherapy and Immunotherapy. *Adv. Mater.* **2023**, *35*, 2210267.

(18) Wang, C.; Liu, X.; Wulf, V.; Vázquez-González, M.; Fadeev, M.; Willner, I. DNA-Based Hydrogels Loaded with Au Nanoparticles or Au Nanorods: Thermoresponsive Plasmonic Matrices for Shape-Memory, Self-Healing, Controlled Release, and Mechanical Applications. *ACS Nano* **2019**, *13*, 3424−3433.

(19) Cangialosi, A.; Yoon, C.; Liu, J.; Huang, Q.; Guo, J. K.; Nguyen, T. D.; Gracias, D. H.; Schulman, R. DNA Sequence-Directed Shape Change of Photopatterned Hydrogels via High-Degree Swelling. *Science* **2017**, *357*, 1126−1129.

(20) Murakami, Y.; Maeda, M. DNA-Responsive Hydrogels That Can Shrink or Swell. *Biomacromolecules* **2005**, *6*, 2927−2929.

(21) Merindol, R.; Martin, N.; Beneyton, T.; Baret, J. C.; Ravaine, S. Fast and Ample Light Controlled Actuation of Monodisperse All-DNA Microgels. *Adv. Funct. Mater.* **2021**, *31*, 2010396.

(22) Zhao, Z.; Wang, C.; Yan, H.; Liu, Y. Soft Robotics Programmed with Double Crosslinking DNA Hydrogels. *Adv. Funct. Mater.* **2019**, *29*, 1905911.

(23) Hu, Y. W.; Kahn, J. S.; Guo, W. W.; Huang, F. J.; Fadeev, M.; Harries, D.; Willner, I. Reversible Modulation of DNA-Based Hydrogel Shapes by Internal Stress Interactions. *J. Am. Chem. Soc.* **2016**, *138*, 16112−16119.

(24) Um, S. H.; Lee, J. B.; Park, N.; Kwon, S. Y.; Umbach, C. C.; Luo, D. Enzyme-Catalysed Assembly of DNA Hydrogel. *Nat. Mater.* **2006**, *5*, 797−801.

(25) Du, X. X.; Bi, Y. H.; He, P. P.; Wang, C. Y.; Guo, W. W. Hierarchically Structured DNA-Based Hydrogels Exhibiting Enhanced Enzyme-Responsive and Mechanical Properties. *Adv. Funct. Mater.* **2020**, *30*, 2006305.

(26) King, J. T.; Shakya, A. Phase Separation of DNA: From Past to Present. *Biophys. J.* **2021**, *120*, 1139−1149.

(27) Jain, A.; Vale, R. D. RNA Phase Transitions in Repeat Expansion Disorders. *Nature* **2017**, *546*, 243−247.

(28) Vieregg, J. R.; Lueckheide, M.; Marciel, A. B.; Leon, L.; Bologna, A. J.; Rivera, J. R.; Tirrell, M. V. Oligonucleotide-Peptide Complexes: Phase Control by Hybridization. *J. Am. Chem. Soc.* **2018**, *140*, 1632−1638.

(29) Lee, C.; Do, S.; Lee, J. Y.; Kim, M.; Kim, S. M.; Shin, Y.; Kim, D. Formation of Non-Base-Pairing DNA Microgels Using Directed Phase Transition of Amphiphilic Monomers. *Nucleic Acids Res.* **2022**, *50*, 4187−4196.

(30) Baeza, I.; Gariglio, P.; Rangel, L. M.; Chavez, P.; Cervantes, L.; Arguello, C.; Wong, C.; Montanez, C. Electron-Microscopy and Biochemical-Properties of Polyamine-Compacted DNA. *Biochemistry-Us* **1987**, *26*, 6387−6392.

(31) Cho, S. K.; Kwon, Y. J. Polyamine/DNA Polyplexes with Acid-Degradable Polymeric Shell as Structurally and Functionally Virus-Mimicking Nonviral Vectors. *J. Controlled Release* **2011**, *150*, 287−297.

(32) Shim, M. S.; Kwon, Y. J. Dual Mode Polyspermine with Tunable Degradability for Plasmid DNA and siRNA Delivery. *Biomaterials* **2011**, *32*, 4009−4020.

(33) Adams, F.; Zimmermann, C. M.; Baldassi, D.; Pehl, T. M.; Weingarten, P.; Kachel, I.; Kraenzlein, M.; Jürgens, D. C.; Braubach, P.; Alexopoulos, I.; Wygrecka, M.; Merkel, O. M. Pulmonary siRNA

https://doi.org/10.1021/acsami.3c17633
ACS Appl. Mater. Interfaces 2024, 16, 24162−24171

Delivery with Sophisticated Amphiphilic Poly(Spermine Acrylamides) for the Treatment of Lung Fibrosis. *Small* **2023**, 2308775.
(34) Mayama, H.; Nakai, T.; Takushi, E.; Tsujii, K.; Yoshikawa, K. Marked Differences in Volume Phase Transitions between Gel and Single Molecule in DNA. *J. Chem. Phys.* **2007**, *127*, 034901.
(35) Costa, D.; Valente, A. J. M.; Miguel, M. G.; Queiroz, J. Plasmid DNA Microgels for a Therapeutical Strategy Combining the Delivery of Genes and Anticancer Drugs. *Macromol. Biosci* **2012**, *12*, 1243−1252.
(36) Merindol, R.; Delechiave, G.; Heinen, L.; Catalani, L. H.; Walther, A. Modular Design of Programmable Mechanofluorescent DNA Hydrogels. *Nat. Commun.* **2019**, *10*, 528.
(37) Yao, C.; Zhang, R.; Tang, J. P.; Yang, D. Y. Rolling Circle Amplification (RCA)-Based DNA Hydrogel. *Nat. Protoc* **2021**, *16*, 5460−5483.
(38) Strekowski, L.; Wilson, B. Noncovalent Interactions with DNA: An Overview. *Mutat Res-Fund Mol. M* **2007**, *623*, 3−13.
(39) Thomas, T. J.; Bloomfield, V. A. Collapse of DNA Caused by Trivalent Cations - pH and Ionic Specificity Effects. *Biopolymers* **1983**, *22*, 1097−1106.
(40) Nguyen, T. T.; Rouzina, I.; Shklovskii, B. I. Reentrant Condensation of DNA Induced by Multivalent Counterions. *J. Chem. Phys.* **2000**, *112*, 2562−2568.
(41) Todd, B. A.; Rau, D. C. Interplay of Ion Binding and Attraction in DNA Condensed by Multivalent Cations. *Nucleic Acids Res.* **2007**, *36*, 501−510.
(42) Oyen, M. L. Mechanical Characterisation of Hydrogel Materials. *Int. Mater. Rev.* **2014**, *59*, 44−59.
(43) Korolev, N.; Lyubartsev, A. P.; Laaksonen, A.; Nordenskiöld, L. On the Competition between Water, Sodium Ions, and Spermine in Binding to DNA: A Molecular Dynamics Computer Simulation Study. *Biophys. J.* **2002**, *82*, 2860−2875.
(44) Ryssy, J.; Lehtonen, A. J.; Loo, J.; Nguyen, M. K.; Seitsonen, J.; Huang, Y. K.; Narasimhan, B. N.; Pokki, J.; Kuzyk, A.; Manuguri, S. DNA-Engineered Hydrogels with Light-Adaptive Plasmonic Responses. *Adv. Funct. Mater.* **2022**, *32*, 2201249.
(45) Li, C.; Rowland, M. J.; Shao, Y.; Cao, T. Y.; Chen, C.; Jia, H. Y.; Zhou, X.; Yang, Z. Q.; Scherman, O. A.; Liu, D. S. Responsive Double Network Hydrogels of Interpenetrating DNA and CB[8] Host-Guest Supramolecular Systems. *Adv. Mater.* **2015**, *27*, 3298−3304.
(46) Chandrasekaran, A. R. Nuclease Resistance of DNA Nanostructures. *Nature Reviews Chemistry* **2021**, *5*, 225−239.
(47) Andersen, O. S. Cellular Electrolyte Metabolism. In *Encyclopedia of Metalloproteins*; Kretsinger, R. H., Uversky, V. N., Permyakov, E. A., Eds.; Springer: New York, 2013; pp 580−587.
(48) Merindol, R.; Loescher, S.; Samanta, A.; Walther, A. Pathway-Controlled Formation of Mesostructured All-DNA Colloids and Superstructures. *Nat. Nanotechnol.* **2018**, *13*, 730−738.

https://doi.org/10.1021/acsami.3c17633
ACS Appl. Mater. Interfaces 2024, 16, 24162−24171